Electronic Supplementary Material (ESI) for Catalysis Science & Technology.

Supporting Information

Surface Defect-Rich g-C_3N_4/TiO_2 Z-scheme Heterojunction for Efficient Photocatalytic Antibiotic Removal: Rational Regulation of Free Radicals and Photocatalytic Mechanism

Pei Ning, Huayu Chen, Jianhui Pan, Junhui Liang, Laishun Qin, Da Chen*, Yuexiang Huang*

College of Materials and Chemistry, China Jiliang University, Hangzhou 310018, Zhejiang, China

*Authors to whom correspondence should be addressed.
Email: hychen@cjlu.edu.cn; dchen_80@hotmail.com

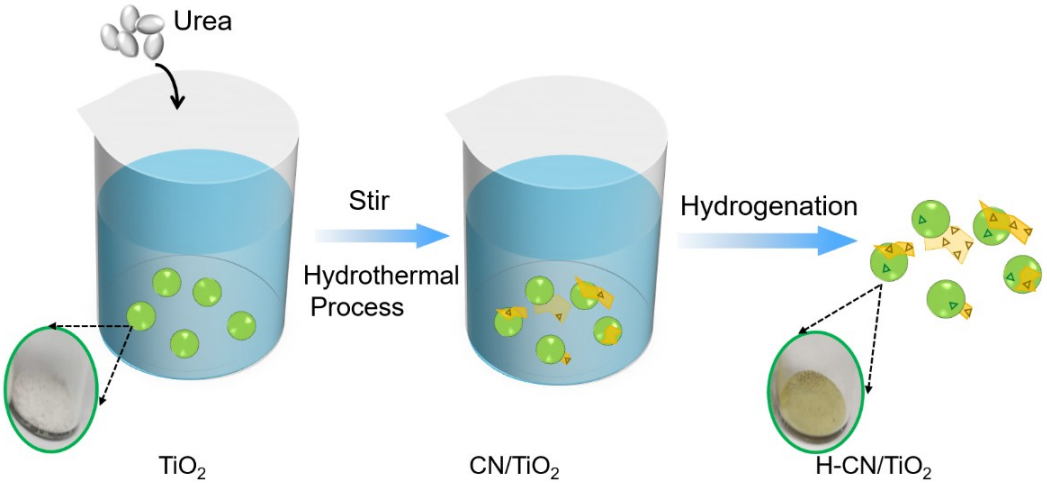

Figure S1. Schematic illustration of preparation of defect-rich H-CN/TiO_2 Z-scheme heterojunction.

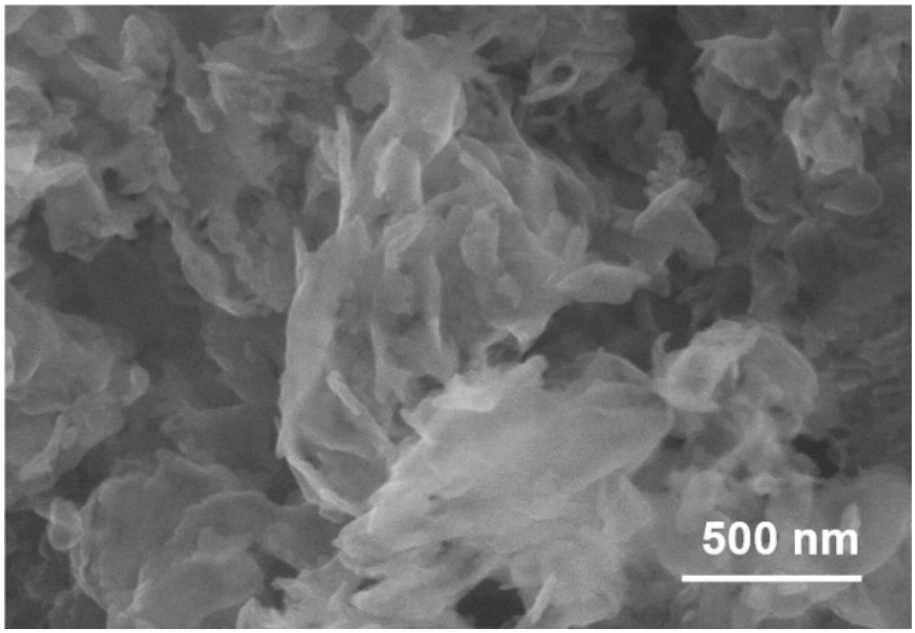

Figure S2. SEM image of the pure g-C_3N_4.

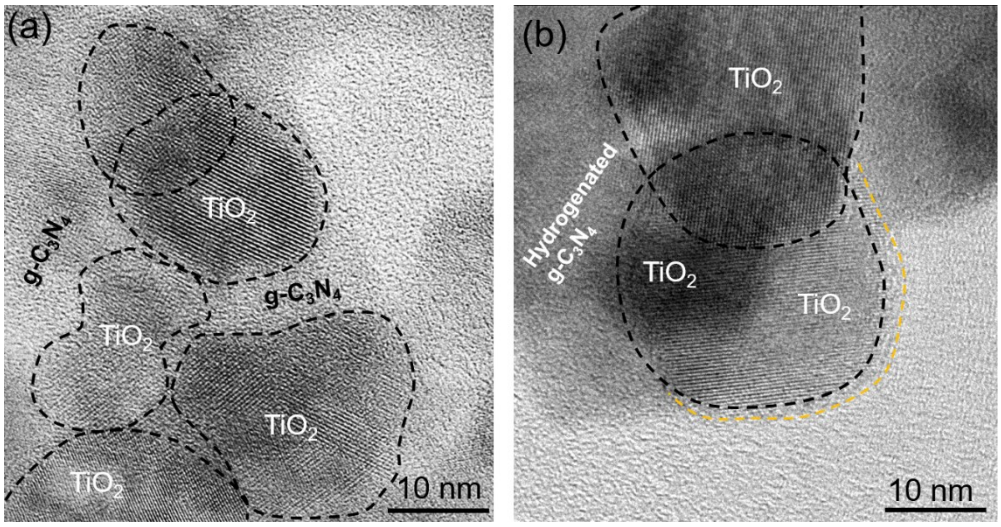

Figure S3. TEM images of (a) CN/TiO_2 and (b) H-CN/TiO_2.

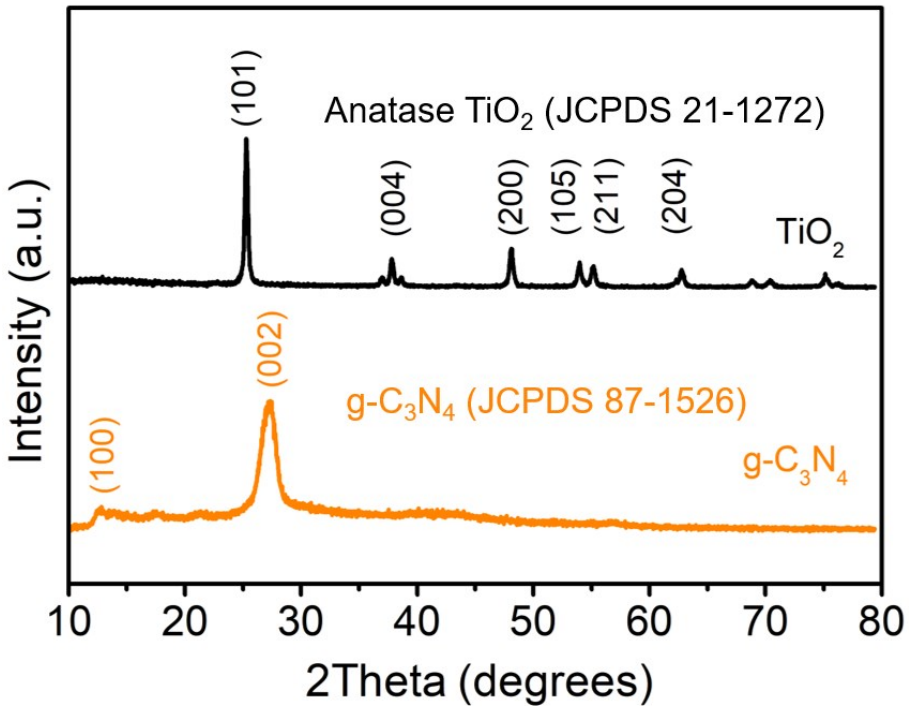

Figure S4. XRD patterns of the pure TiO_2 and g-C_3N_4.

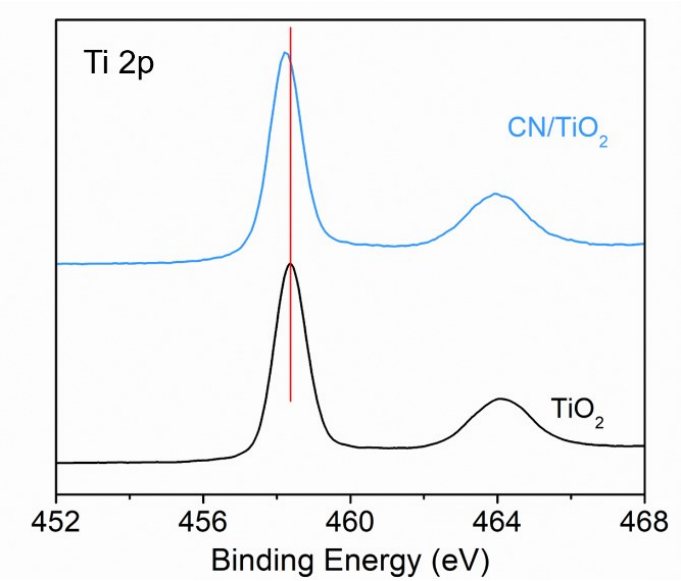

Figure S5. Ti 2p XPS spectra of the TiO_2 and CN/TiO_2.

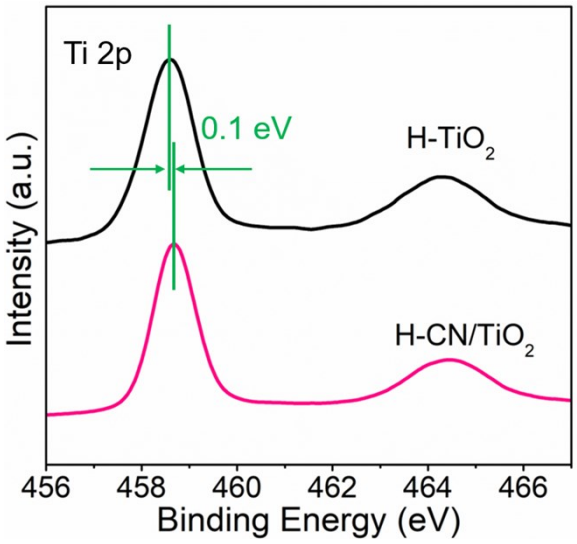

Figure S6. High-resolution XPS spectra of Ti 2p level for the $H\text{-}TiO_2$ and $H\text{-}CN/TiO_2$ composite.

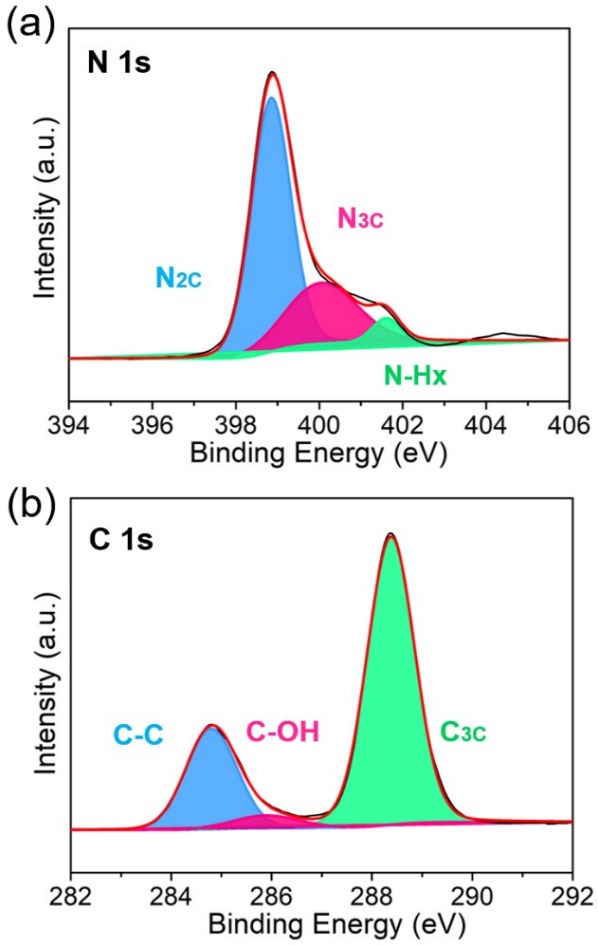

Figure S7. XPS spectra of N 1s (a) and C 1s (b) for the pure g-C_3N_4.

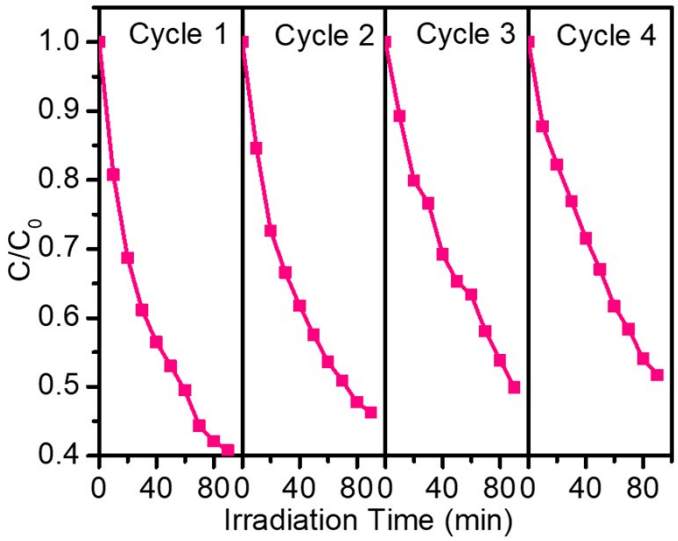

Figure S8. Photocatalytic degradation of TC-HCl over the H-CN/TiO_2 sample for four cycles

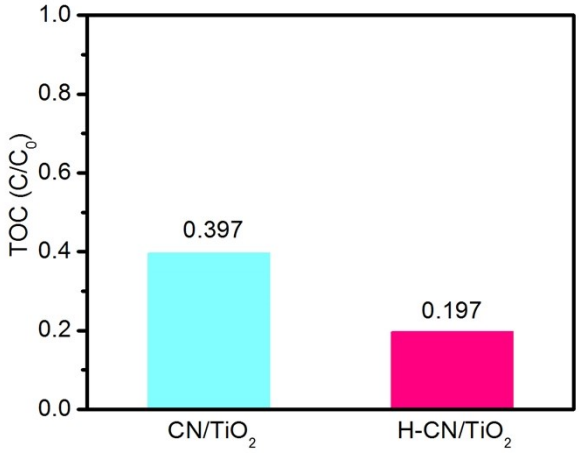

Figure S9. TOC removal experiments over the CN/TiO_2 and H-CN/TiO_2 after degradation for 90 min.

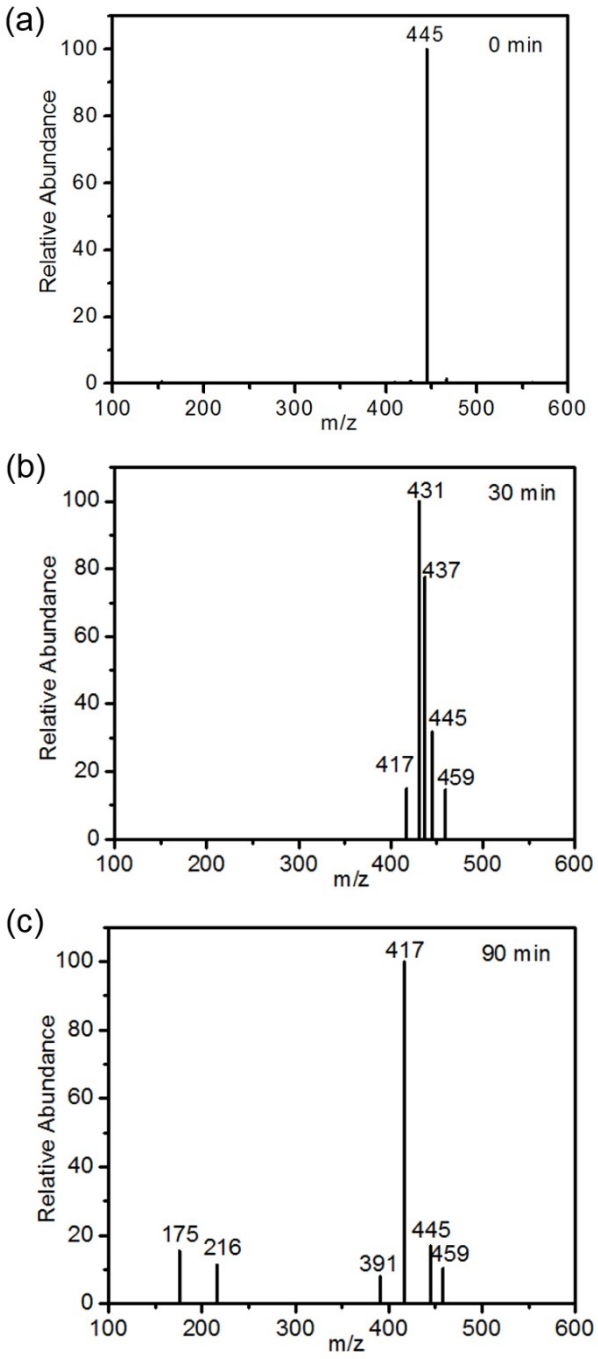

Figure S10. m/z values of TC-HCl degradation over the H-CN/TiO_2: (a)initial TC-HCl solution and TC-HCl solution after degradation for (b) 30 and (c) 90 min.

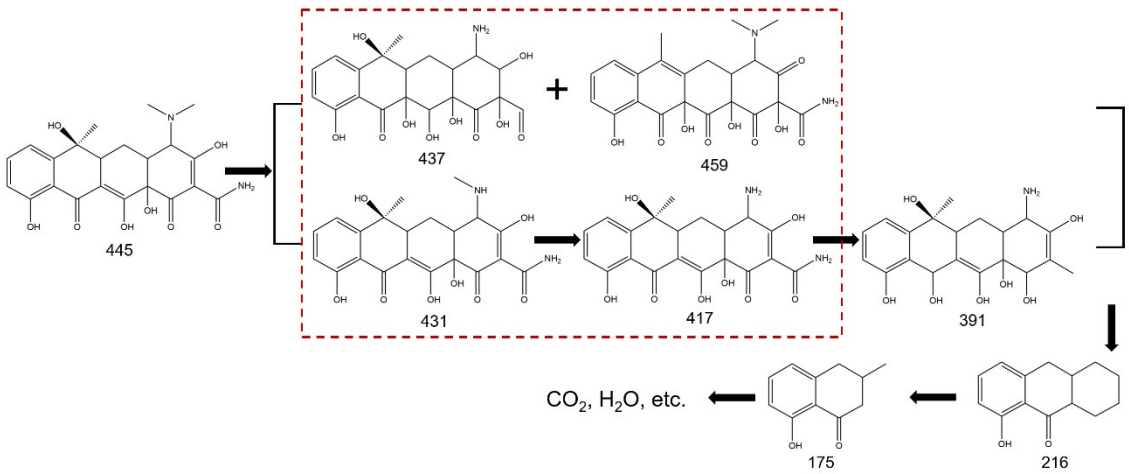

Figure S11. Possible degradation pathway and intermediate products of TC-HCl during the degradation process.

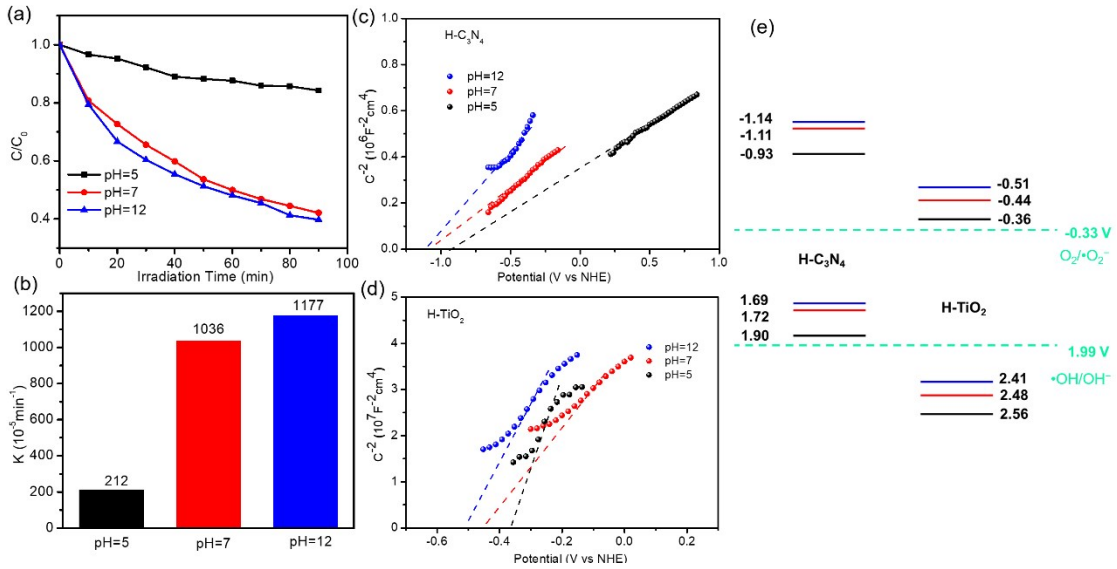

Figure S12. (a) The degradation dynamic curves and (b) rate constants of the H-CN/TiO_2 for TC-HCl degradation under different pH environments. Mott-Schottky measurements of (c) H-C_3N_4 and (d) H-TiO_2 under different pH environments. (e) Schematic illustration of the energy bandgap positions of the H-CN/TiO_2 under different pH environments (pH = 5, 7 and 12)

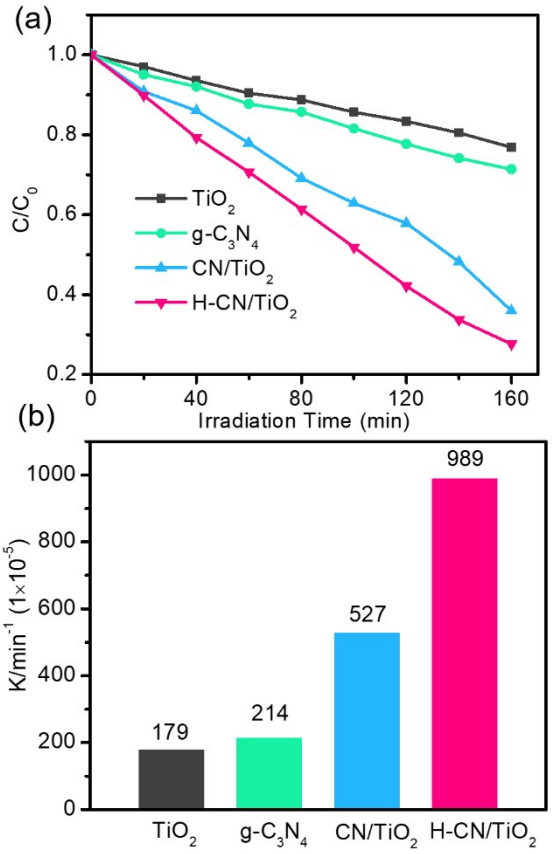

Figure S13. (a) The dynamic curves and (b) rate constants of the samples for photocatalytic RhB degradation under the irradiation of 300 W Xe arc lamp equipped with an L42 cutoff filter.

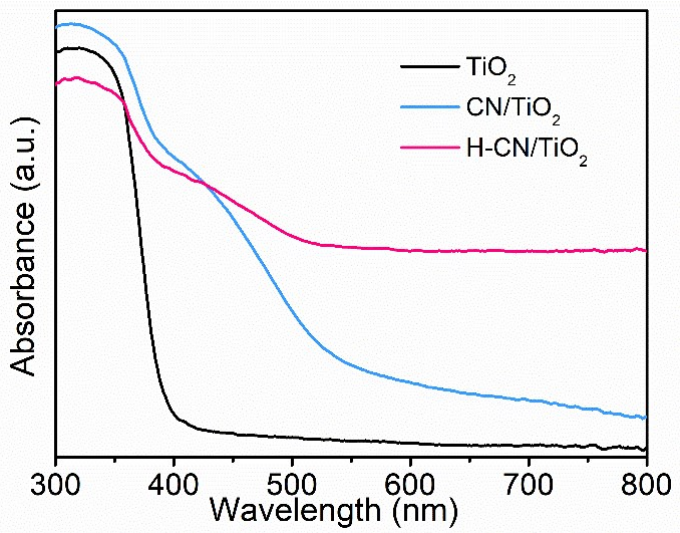

Figure S14. UV-visible absorption spectra of the samples.

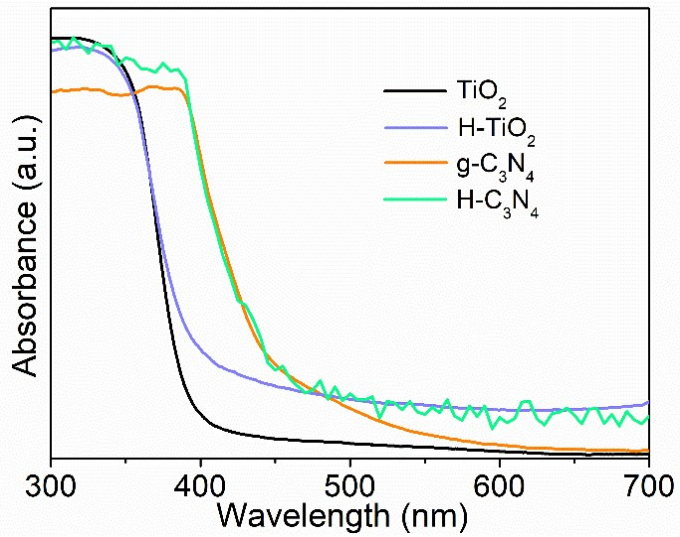

Figure S15. UV-visible absorption spectra of the samples before and after hydrogenation.

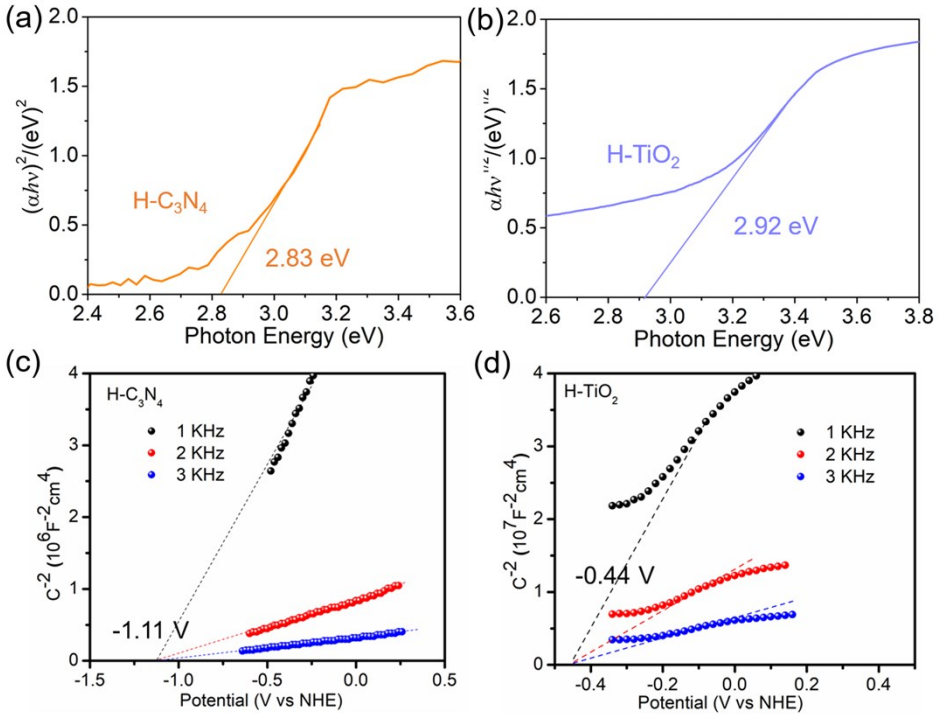

Figure S16. The plots of the $(\alpha h\nu)^n$ versus photon energy ($h\nu$) of (a) H-C_3N_4 and (b) H-TiO_2. Mott-Schottky plots of (c) H-C_3N_4 and (d) H-TiO_2.

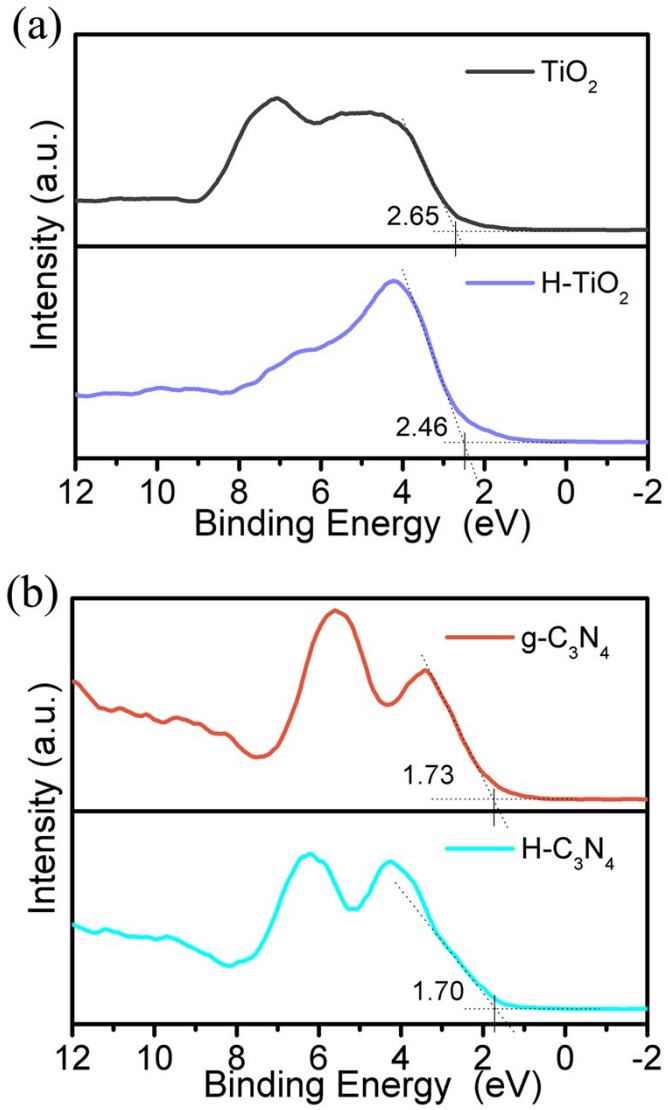

Figure S17. XPS valence band spectra of the TiO_2, H-TiO_2, g-C_3N_4 and H-C_3N_4 samples.

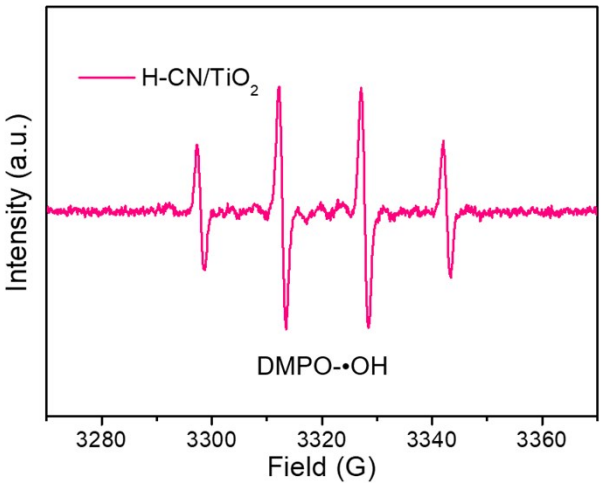

Figure S18. EPR spectra of the H-CN/TiO_2 Z-scheme heterojunction for DMPO-•OH under Xe lamp + L42 cutoff filter.

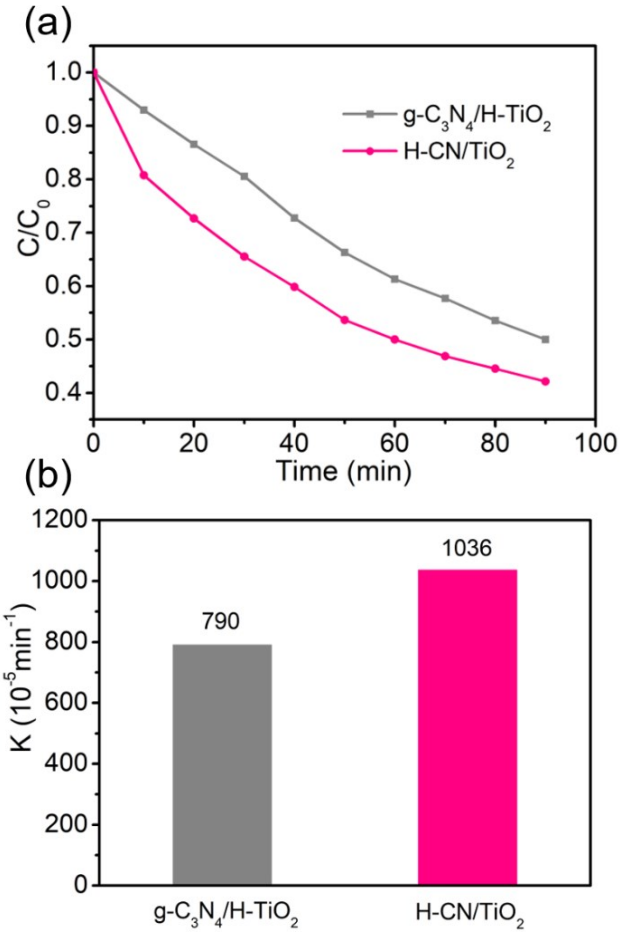

Figure S19. (a) Degradation dynamic curves and (b) rate constants of the g-C_3N_4/H-TiO_2 and H-CN/TiO_2 samples.

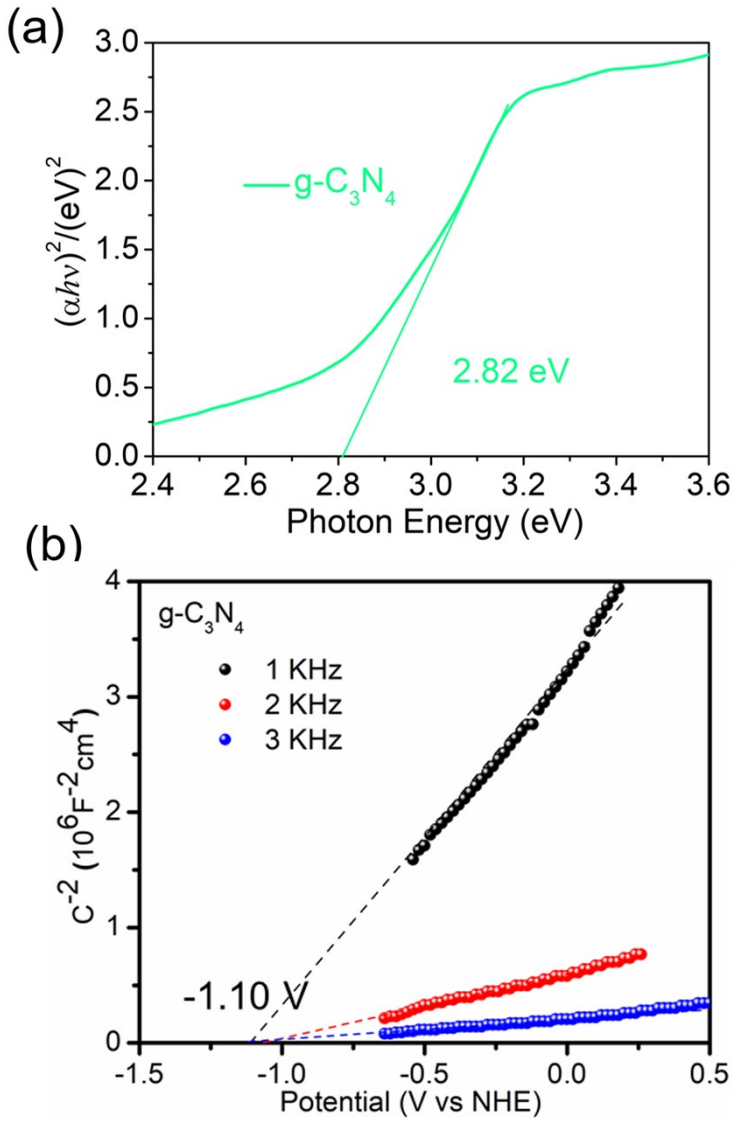

Figure S20. (a) The plot of the $(\alpha h\nu)^n$ versus photon energy ($h\nu$) and (b) Mott-Schottky measurement of the g-C_3N_4.

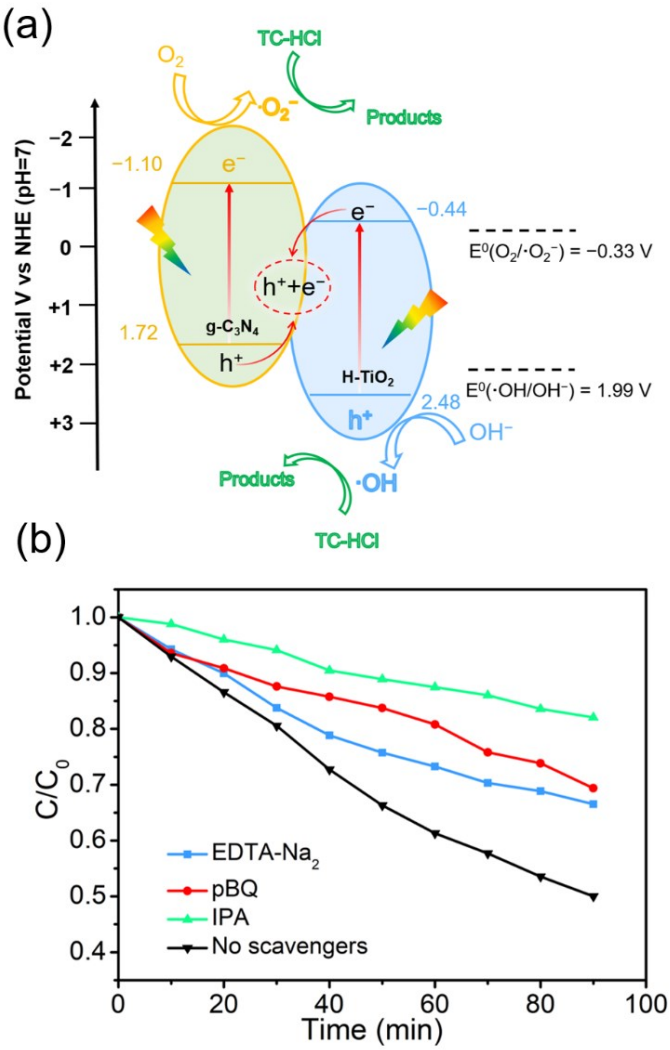

Figure S21. (a) Possible photodegradation mechanism of TC-HCl over the Z-scheme the g-C_3N_4/H-TiO_2 heterojunction. (b) Photodegradations over the g-C_3N_4/H-TiO_2 with scavengers of different reactive species (300 W Xe arc lamp + L42 cutoff filter).

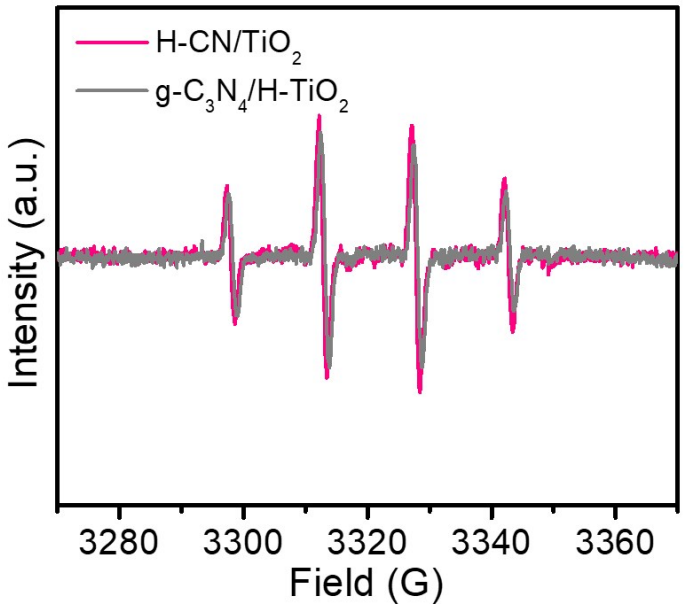

Figure S22. EPR spectra of the g-C_3N_4/H-TiO_2 and H-CN/TiO_2 heterojunctions for DMPO-•OH under Xe lamp + L42 cutoff filter.

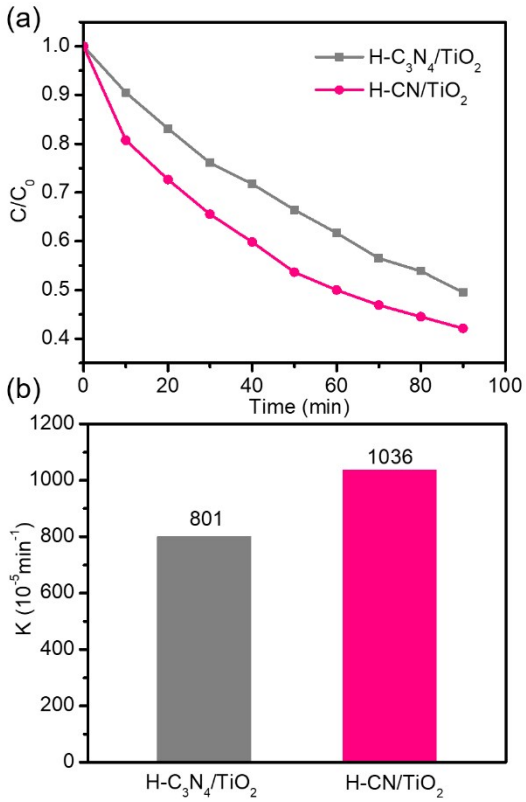

Figure S23. (a) Degradation dynamic curves and (b) rate constants of the H-C_3N_4/TiO_2 and H-CN/TiO_2 samples.

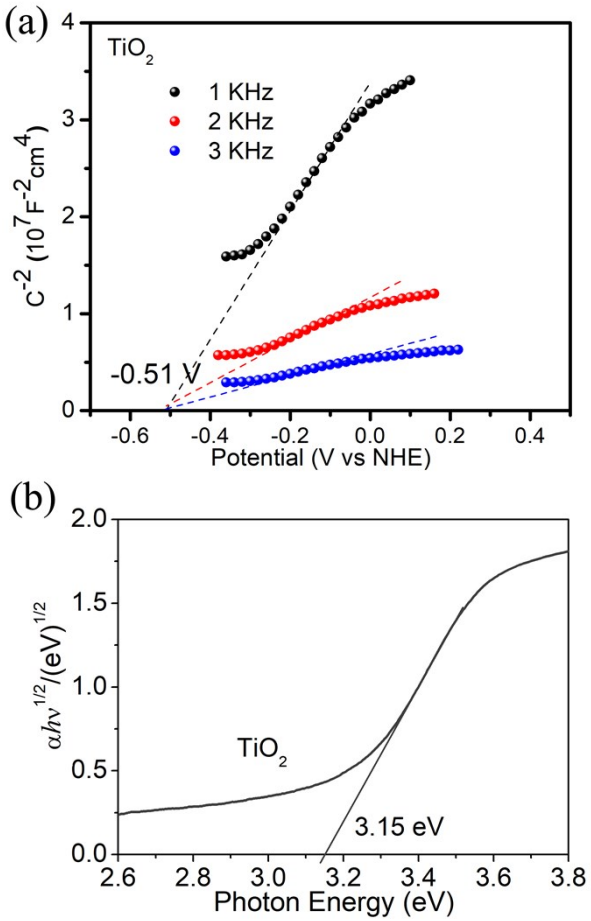

Figure S24. (a) Mott-Schottky measurement and (b) the plot of the $(\alpha h\nu)^n$ versus photon energy ($h\nu$) of the TiO_2.

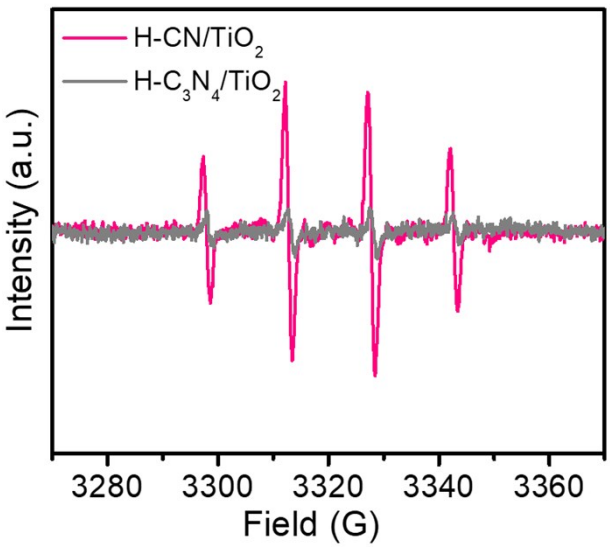

Figure S25. EPR spectra of the H-C_3N_4/TiO_2 and H-CN/TiO_2 heterojunctions for DMPO-•OH under Xe lamp + L42 cutoff filter.

Table S1. Ratios of N_{2C} to N_{3C} of the samples (from XPS data).

Sample	***g-C_3N_4***	***CN/TiO_2***	***H-CN/TiO_2***
N_{2C}/N_{3C}	2.38	0.891	0.374

Table S2. Element compositions and ratios of the heterojunctions (from XPS data).

Element	***C (at.%)***	***N (at.%)***	***N/C (atomic ratio)***
CN/TiO_2	18.5	0.92	0.0497
H-CN/TiO_2	25.8	0.88	0.0341